Angle Resolved Relaxation of Spin Currents by Antiferromagnets in Spin Valves

D. M. Polishchuk [1,2,*] A. Kamra,[3] T. I. Polek,[2] A. Brataas,[3] and V. Korenivski[1]

[1]*Nanostructure Physics, Royal Institute of Technology, 10691 Stockholm, Sweden*
[2]*Institute of Magnetism, NASU and MESU, 03142 Kyiv, Ukraine*
[3]*Center for Quantum Spintronics, Department of Physics, Norwegian University of Science and Technology, NO-7491 Trondheim, Norway*

We observe and analyze tunable relaxation of a pure spin current by an antiferromagnet in spin valves. This is achieved by carefully controlling the angle between a resonantly excited ferromagnetic layer pumping the spin current and the Néel vector of the antiferromagnetic layer. The effect is observed as an angle-dependent spin-pumping contribution to the ferromagnetic resonance linewidth. An interplay between spin-mixing conductance and, often disregarded, longitudinal spin conductance is found to underlie our observations, which is in agreement with a recent prediction for related ferromagnetic spin valves.

Spin polarization of the conduction electrons in metallic ferromagnets enables external control of the electrical properties of magnetic multilayers via the relative magnetization orientation of the ferromagnetic layers comprising the multilayer. The resulting angle-dependent transmission of a spin-polarized current is behind prominent effects such as giant [1,2] and tunneling [3] magnetoresistance (MR) as well as spin transfer torques [4], which paved the way for rapidly developing spin electronics [5,6].

The related angle-dependent dissipation of spin currents is behind the anisotropic [7,8] and spin-Hall MR [9–11] observed in heavy-metal–antiferromagnet (HM-AF) bilayers [12,13]. The key characteristic shared by these two effects is the change in the bilayer's resistance dependent on whether the polarization of the spin current in the HM is collinear or orthogonal to the axis of preferred spin alignment in the AF (its Néel vector **N**). The demonstrated feasibility of controlling spin currents in antiferromagnetic nanostructures indicates a considerable potential of the emerging field of antiferromagnetic spintronics [14–17]. However, an explicit, angle-resolved experimental study of the interaction between a spin current and the Néel vector of an AF, as well as its functional form and physical parameter space, that would underpin the existing strong theoretical effort [18–20] is still pending.

Ferromagnetic resonance (FMR) driven spin pumping is a unique tool for analyzing spin relaxation in ferromagnet–nonmagnet–static-ferromagnet (F-N-F_{st}) [21–25] and

ferromagnet-nonmagnet-antiferromagnet (F-N-AF) [26–29] spin valves. The ferromagnetic layer F is the source as well as the probe of a pure spin current pumped into the nonmagnetic spacer N and static ferromagnetic F_{st} or AF layers. Since there is negligible spin dissipation in the typically nm-thin spacer N, spin pumping probes the spin relaxation due to the static F_{st} or AF layers measured via the backflow spin-current contribution to the FMR linewidth of F. If the spin absorption by the static layer is anisotropic, the spin-pumping contribution is manifested as an angle-dependent modulation of the FMR linewidth. Indeed, anisotropic absorption of pure spin currents was reported for F-N-F_{st} [21,25]. Reference [21] exploited the spin pumping current-mediated dynamical exchange between the two F layers in achieving an angle-dependent FMR linewidth. On the other hand, Ref. [25] exploited the magnetization orientation-dependent intrinsic damping of the F_{st} layer for obtaining a corresponding damping dependence in the F layer. In both works, however, the magnetic moments of the spin-source F layer and the spin-sink F_{st} layer were essentially collinear. To the best of our knowledge, the anisotropy of spin relaxation studied by controllably varying the angle between the spin-current polarization (set by F) and the magnetic axis of F_{st} or AF has not been demonstrated in magnetic multilayers. The main difficulty in achieving a reliable control of the noncollinear alignment in such spin valve structures lies in the presence of a kOe-range external magnetic field required in a typical FMR experiment, which often fully aligns the studied multilayer magnetically.

In this Letter, we demonstrate controllable magnetic damping in a F layer via ϕ-dependent interaction of the emitted spin pumping current with the Néel vector of an AF layer in a F-N-AF-F_p type spin valve, where ϕ is the angle between the equilibrium magnetization in F and the AF Néel vector. Carrying out detailed ϕ-dependent,
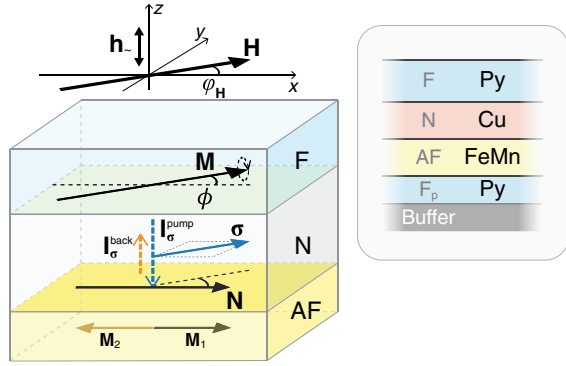
FIG. 1. Schematic of the studied multilayer and the FMR measurement configuration when external magnetic field **H** is applied in the film plane xy. The equilibrium axis of resonating magnetization **M** in F follows the external field **H**, whereas the AF vector **N** is fixed in the xy plane (using, e.g., a ferromagnetic seed layer, F_p; inset). Vector **N** forms angle ϕ with polarization σ of spin-pumped current $\mathbf{I}_s^{\text{pump}}$.

variable-temperature measurements of the FMR-driven, spin-pumping-mediated magnetization damping, we observe a pronounced maximum when the magnetization of F is orthogonal to the AF Néel vector. Our results are well described by a theoretical model analogous to that for ferromagnetic spin valves [30] and indicate the dominance of longitudinal over spin-mixing conductance in spin relaxation by the AF layer. This consistence with the recent prediction [30] highlights the importance of longitudinal spin transport in magnetic multilayers and establishes an important pathway towards achieving *in situ* damping tunability.

Spin pumping experiment.—Spin pumping is an emission of spin angular momentum ($\mathbf{I}_\sigma^{\text{pump}}$) by a resonantly precessing ferromagnet (F) into an adjacent nonmagnetic spacer N [31]. In this sense, spin pumping is a reciprocal effect to a spin-transfer torque [32]. $\mathbf{I}_\sigma^{\text{pump}}$ carries spin away from F, which increases the magnetization damping in F, usually detected as a broadening of the F layer's FMR linewidth [33,34]. Considering the F-N-AF trilayer used in this work, and taking spin relaxation in N to be negligible, a fraction of the spin-pumping current is reflected at the N-AF interface and returns back to F. The spin-pumping contribution to the FMR linewidth is proportional to the difference between $\mathbf{I}_\sigma^{\text{pump}}$ and the back-flow spin current $\mathbf{I}_\sigma^{\text{back}}$ (Fig. 1) [32]. A change in the relative orientation between the spin-current polarization σ and the AF's Neel vector should affect $\mathbf{I}_\sigma^{\text{back}}$, thereby, modulating the FMR linewidth of F.

The F-N-AF trilayer under "in-plane" FMR, illustrated in Fig. 1, has the equilibrium orientation of the resonating magnetization in magnetically soft F (**M**) aligned with the external magnetic field ($\simeq 1$ kOe) applied at angle $\varphi_{\mathbf{H}}$. At the same time, the Néel vector **N** of AF is essentially insensitive to this relatively weak field and remains directionally fixed, provided it is suitably set in fabrication (as

detailed below). The spin valve structure allows one to control the angle ϕ between the F layer magnetization and the AF layer Néel vector enabling us to extract the ϕ dependence of the spin-pumping contribution to the FMR linewidth.

A macroscopic magnetic anisotropy in AF—the key AF property for this study—can be induced by deposition in a static magnetic field and/or postfabrication magnetic annealing [35]. The other effective approach is to deposit a thin AF layer onto a saturated ferromagnetic seed layer (F_p), which induces a strong exchange bias in the AF-F_p bilayer. The latter results in a pronounced unidirectional magnetic anisotropy in F_p as well as a magnetic axis in AF. We have fabricated a series of multilayers, where anti-ferromagnetic FeMn is grown on either a ferromagnetic (Py) or nonmagnetic (Ta) seed layer. Here, FeMn and Py denote $Fe_{50}Mn_{50}$ and $Fe_{20}Ni_{80}$ (Permalloy) alloys. By studying a series of samples with differently thick FeMn ($t = 3, 5,$ and 7 nm) [36], the thickness of the FeMn layer of 7 nm was found to be optimal as regards a strong directional exchange bias throughout the FeMn/Py bilayer with a high blocking temperature ($T_b \approx 420$ K) [35,37]. The opposite surface of the FeMn layer, acting as the spin-current reflector or sink, is interfaced with the free, soft Py layer via a nonmagnetic Cu spacer. The thickness of the Cu layer (6 nm) was chosen much smaller than the spin diffusion length in Cu ($\lambda_s > 100$ nm at room temperature [38]) to ensure negligible spin dissipation in N.

FMR measurements were carried out at a constant frequency of 9.88 GHz while sweeping an external magnetic field **H** applied in the film plane. The obtained spectra exhibit a strong resonance line from the free Py layer, the position of which (the resonance field) reveals a very weak uniaxial magnetic anisotropy in the film plane [Figs. 2(a) and 2(b)]. The latter is often referred to as directional pair-ordering anisotropy in magnetic alloys, which is induced by growth or annealing in magnetic field [39,40]. The FMR spectra for the structures with the FeMn/Py bilayer exhibit an additional resonance line, which we attribute to the seed Py layer and use as an independent probe of the magnetic directionality of AF. This line exhibits a pronounced unidirectional anisotropy, indicating a strong exchange bias in the FeMn/Py bilayer [35].

Angle-dependent FMR linewidth.—The FMR linewidth of the free Py layer ΔH as well as the resonance field H_r were obtained by fitting the spectra with a Dysonian [41]. ΔH versus $\varphi_{\mathbf{H}}$ for the samples with the magnetic and nonmagnetic seed layers differ significantly in the magnitude of the variation as well as its angular profile [Fig. 2(c)]. On the other hand, the respective resonance fields $H_r(\varphi_{\mathbf{H}})$ show the same behavior [Fig. 2(b)], indicating that the saturation magnetization and the magnetic anisotropy of the free layer are largely unaffected by the seed layer. The observed difference in the magnetic damping (ΔH) for the two structures must, therefore, be attributed to a difference in the magnetic state of their respective FeMn layers. The
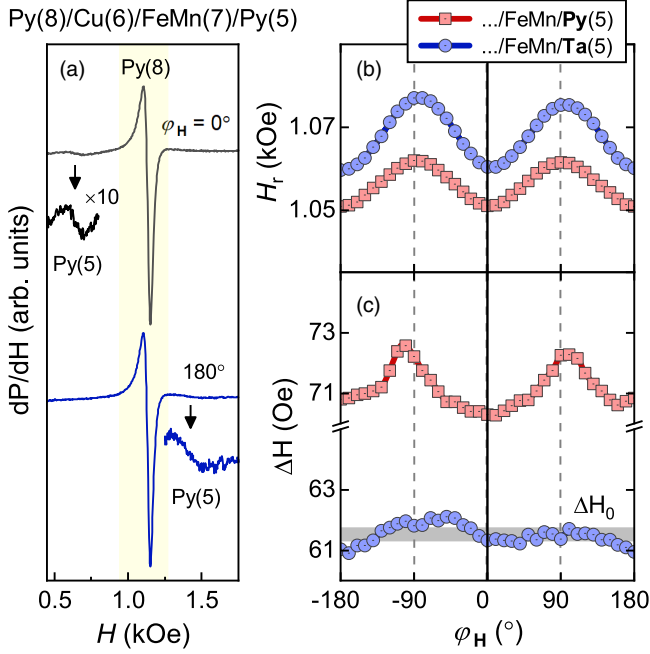
FIG. 2. (a) In-plane FMR spectra measured along (0°) and opposite (180°) to the exchange-pinning direction set by the seed Py(5) layer. (b), (c) Angular dependence of the resonance field (H_r) and the linewidth (ΔH) for the free Py(8) layer for the structures where the antiferromagnetic FeMn layer was grown on nonmagnetic Ta(5) or ferromagnetic Py(5). The data were measured at 280 K.

FIG. 3. (a) Angle-dependent spin-pumping contribution ($\Delta H - \Delta H_0$) versus $\varphi_{\mathbf{H}}$, obtained from the measured FMR linewidth by subtracting the predominantly isotropic linewidth for the control sample (FeMn/Ta-based) at each given temperature. Solid lines are the fits to theory [Eq. (1)]. (b) Corresponding angle dependences of H_r. Solid lines are the fit using the standard FMR phenomenology. (c) Illustration of the rotating torque on the AF with Néel vector $\mathbf{N}$ by the exchange-coupled Py(5) layer of magnetization $\mathbf{M}_p$, for two characteristic temperatures. (d) Extracted from the fitting in (a), the temperature dependence of the spin-relaxation asymmetry parameter.

essentially isotropic behavior of ΔH for the case of FeMn/ Ta indicates that the FeMn layer exhibits no macroscopic magnetic axis as antiferromagnetic domains formed on nonmagnetic Ta are likely to orient randomly. In contrast, the pronounced anisotropy of ΔH for the structure with the FeMn/Py bottom magnetic layer is evidence for a well-defined macroscopic magnetic anisotropy in the FeMn layer, the conclusion additionally and independently supported by the observed pronounced unidirectional anisotropy in the seed-Py layer [36]. In what follows, we focus on this key result of anisotropic spin relaxation in the FeMn/Py-based structure.

The multilayers with FeMn/Py exhibit a thermally induced transformation of the ΔH vs $\varphi_{\mathbf{H}}$ profile. The maximum in $\Delta H(\varphi_{\mathbf{H}})$ observed at room temperature at $\varphi_{\mathbf{H}} \approx \pm 90°$ shifts to larger angles with decreasing temperature [Fig. 3(a)]. At the same time, there are no temperature-induced changes in the angle profiles of the resonance field, except the offset in the magnitude of H_r due to the temperature variation in the saturation magnetization of Py [36]. This implies that the observed changes in ΔH vs $\varphi_{\mathbf{H}}$ with temperature are caused by factors external to the free layer—in our case, the spin-pumping-mediated effect of the AF on ΔH—rather than by any changes in the intrinsic magnetic properties of the free layer. Importantly, the changes in the angular profiles of Fig. 3(a) are associated
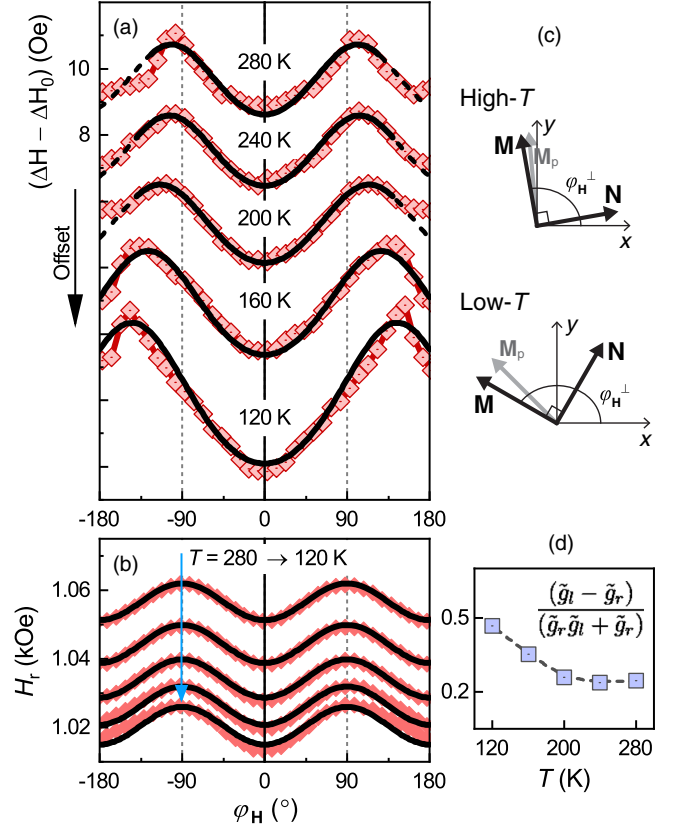
with a temperature dependence of the AF layer pinning by the seed underlayer. This is strongly supported by the corresponding ΔH vs $\varphi_{\mathbf{H}}$ for the FeMn/Ta-based structures, which remain largely isotropic at all temperatures [36].

Spin-pumping contribution.—We explain the observed angle dependence of the FMR linewidth as due to the spin-pumping contribution to the magnetization dynamics of the free layer. We extend the phenomenology of the spin-pumping effect [31,32] to a noncollinear ferromagnetic-nonmagnetic-antiferromagnetic (F-N-AF) trilayer system. The magnetization dynamics of F is described in terms of the spin conductivities of the F-N and N-AF interfaces for an arbitrary mutual orientation of the respective magnetic order parameters—magnetization $\mathbf{M}$ and Néel vector $\mathbf{N}$.

The anisotropic ΔH vs $\varphi_{\mathbf{H}}$ profile, shown in Fig. 2(c), exhibits maxima close to $\varphi_{\mathbf{H}} = \pm 90°$, which can be qualitatively explained as follows. The precessing F pumps

spins into the adjacent spacer layer, a fraction of which is subsequently absorbed by AF. The absorbed spin current manifests as additional damping in F. However, only the component of spin current that is orthogonal to the equilibrium F magnetization determines the damping in it. This component is best absorbed when the F magnetization and the AF Néel vector are mutually orthogonal, provided that AF absorbs and dissipates the longitudinal component stronger than the transverse component of the spin current.

In the general case, the spin-pumping contribution to the integral FMR linewidth can be quantitatively expressed in terms of the spin conductances of the F-N and N-AF interfaces [30]. The other contributions, such as the intrinsic Gilbert damping and inhomogeneous terms, have a much weaker dependence on the in-plane angle and add up in the total $\Delta H(\varphi_{\mathbf{H}})$ to a constant $\Delta H_{\text{int}} \approx \text{const}$ [42]. The case of a noncollinear mutual alignment of $\mathbf{M}$ and $\mathbf{N}$ can be treated in a manner analogous to Ref. [30]. The full FMR linewidth becomes

$$\Delta \tilde{H} = \Delta \tilde{H}_0 + 0.5 \frac{\tilde{g}_r \tilde{g}_l}{(\tilde{g}_r \tilde{g}_l + \tilde{g}_r) + (\tilde{g}_l - \tilde{g}_r)\cos^2\phi}, \quad (1)$$

where $\Delta \tilde{H} = \Delta H(4\pi MV)/(g_r^{\star} \hbar \omega)$, ω—the frequency of the applied microwave field, V—the film volume; $\tilde{g}_{l,r} = g_{l,r}/g_r^{\star}$, where the longitudinal spin conductance (g_l) and the real part of the spin-mixing conductance (g_r) characterise the N-AF subsystem, whereas $g_r^{\star}$ relates to the F-N interface. The second term in (1) is the angle-dependent spin-pumping contribution, a function of angle ϕ between $\mathbf{M}$ and $\mathbf{N}$. $\Delta \tilde{H}_0$, in turn, consists of $\Delta \tilde{H}_{\text{int}}$ and the angle-independent spin-pumping contribution: $\Delta \tilde{H}_0 = \Delta \tilde{H}_{\text{int}} + 0.5\tilde{g}_r/(1 + \tilde{g}_r)$.

Equation (1) can be used for fitting the experimental ΔH vs $\varphi_{\mathbf{H}}$ data. Subtracting the angle-independent background ΔH_0 from the total ΔH allows one to fit the data using only the second, angle-dependent term in (1). In this respect, and based on the detailed discussion above [Fig. 2(c) and related text], the most appropriate is to take as ΔH_0 the linewidth for the FeMn/Ta-based structure, in fact, specifically designed for this calibration. Figure 3(a) shows the result, which agrees well with the experiment.

Effect of temperature.—With changing temperature, the anisotropic spin relaxation undergoes a transformation of its angular form [Fig. 3(a)], which can be explained by the temperature-dependent properties of the exchange-pinned AF-F_p bilayer. The stronger interface exchange pinning at lower temperatures results in a stronger torque on the AF, such that $\mathbf{M}$ and $\mathbf{N}$ become orthogonal at different angles of the applied in-plane field (of fixed magnitude $H = H_r^{\text{F}} = 1.03–1.08$ kOe) for different temperatures, as detailed below.

With decreasing temperature, the maximum in ΔH shifts from $\varphi_{\mathbf{H}} \approx \pm 90°$ to larger angles [Fig. 3(a)], whereas the peak in H_r remains in the same position at $90°$ [Fig. 3(b)]. The shift of ΔH can be explained by a deviation of vector $\mathbf{N}$

(tilt angle $\varphi_{\mathbf{N}}$) from its easy (exchange-pinning) direction, so the $90°$ rotation of $\mathbf{M}$ with respect to $\mathbf{N}$ occurs at a larger $\varphi_{\mathbf{H}}$ [field angle measured from the exchange-pinning direction, as illustrated in Figs. 3(c)]. This tilt of $\mathbf{N}$, increasing at low temperatures for a given field torque (acting via F_p), is due to the well-known strengthening of the exchange coupling between AF and F_p (increasing from about AF's T_N toward low temperature). The magnetization $\mathbf{M}_p$ of F_p follows the direction of the applied magnetic field $\mathbf{H}$ (the applied ≈ 1 kOe exceeds the exchange-pinning field at all temperatures) and, via the exchange at the interface, torques $\mathbf{N}$ off the initial equilibrium orientation ($\varphi_{\mathbf{N}} = 0$). This tilting is quantitatively described by a competition between the exchange bias in the AF-F_p bilayer (J_{ex}) and the Zeeman energy of F_p (J_Z), as detailed in [36]. With changing temperature, J_Z varies slowly since the Curie point of F_p is much higher than the experimental temperature range, whereas J_{ex} has a pronounced temperature dependence [36]: the extracted $J_{\text{ex}} \approx 0.3$ erg/cm^2 at 200 K vanishes toward the Néel point of the AF (more precisely the blocking point, $T_b \approx T_N$ [35]).

Equation (1) fits the measured data very well for all temperatures [solid lines in Fig. 3(a)], when modified according to the discussion above, such that angle ϕ between $\mathbf{M}$ and $\mathbf{N}$ is scaled by a temperature-dependent parameter reflecting the tilt of the AF, $\phi = (\varphi_{\mathbf{H}} - \varphi_{\mathbf{N}}) = a\varphi_{\mathbf{H}}$ ($a \leq 1$). An additional analysis of the resonance of the seed Py layer based on the relevant simulations [36] shows that the AF tilt angle $\varphi_{\mathbf{N}}$ is linear in $\varphi_{\mathbf{H}}$ in the angle interval slightly wider than that between the two maxima in $\Delta H(\varphi_{\mathbf{H}})$. The parts of the calculated curves outside this fitting interval are dashed in Fig. 3(a). The final result of the analysis is the parameter representing the anisotropic magnetization damping, which is proportional to the difference $(g_l - g_r)$ [Fig. 3(b)] and shows how the observed angle-dependent FMR linewidth directly stems from the spin-conductance asymmetry of the N-AF interface.

Discussion and Conclusions.—The result of the above analysis is a finite and positive $(g_l - g_r)$ [Fig. 3(b)], which means that the spin absorbed by the AF at the N-AF interface is larger when the spin-current polarization σ is collinear with the AF's magnetic axis ($\mathbf{x}$) and smaller for orthogonal σ and $\mathbf{x}$. In arriving at this conclusion, we have assumed that the exchange biasing tends to align the Néel vector of the AF with the seed layer's magnetization. This assumption is supported by the widely accepted uncompensated-spin model of exchange bias [43,44] describing the effect in similar metallic AF-F_p bilayers [45]. Therefore, our experiment demonstrates that g_l exceeds g_r in the considered metallic AFs, which is consistent with the strong spin relaxation observed in such AFs [26,27], and is in contrast to the typical assumption, $g_l \ll g_r$, in literature [32,46,47].

Furthermore, the shown sensitivity of the magnetization damping in the resonating F layer to the presence of an

induced magnetic axis in the static AF layer is an example of how spin-pumping can be used for probing the changes in the spin configuration of AFs subjected to external stimuli (thermal and/or magnetic). Finally, the reported angular modulation of the FMR linewidth is an experimental demonstration of an *in situ*, spin-pumping-mediated control of magnetization damping in magnetic multilayers predicted recently [30].

---

*dpol@kth.se.

[1] M. N. Baibich, J. M. Broto, A. Fert, F. Nguyen Van Dau, F. Petroff, P. Etienne, G. Creuzet, A. Friederich, and J. Chazelas, Giant Magnetoresistance of (001)Fe/(001)Cr Magnetic Superlattices, Phys. Rev. Lett. **61**, 2472 (1988).

[2] G. Binasch, P. Grünberg, F. Saurenbach, and W. Zinn, Enhanced magnetoresistance in layered magnetic structures with antiferromagnetic interlayer exchange, Phys. Rev. B **39**, 4828 (1989).

[3] J. S. Moodera, L. R. Kinder, T. M. Wong, and R. Meservey, Large Magnetoresistance at Room Temperature in Ferromagnetic Thin Film Tunnel Junctions, Phys. Rev. Lett. **74**, 3273 (1995).

[4] J. C. Slonczewski, Current-driven excitation of magnetic multilayers, J. Magn. Magn. Mater. **159**, L1 (1996).

[5] Igor Žutić, Jaroslav Fabian, and S. Das Sarma, Spintronics: Fundamentals and applications, Rev. Mod. Phys. **76**, 323 (2004).

[6] *Spin Current*, edited by S. Maekawa, S. O. Valenzuela, E. Saitoh, and T. Kimura, 2nd ed. (Oxford University Press, Oxford, 2017).

[7] B. G. Park, J. Wunderlich, X. Martí, V. Holý, Y. Kurosaki, M. Yamada, H. Yamamoto, A. Nishide, J. Hayakawa, H. Takahashi, A. B. Shick, and T. Jungwirth, A spin-valve-like magnetoresistance of an antiferromagnet-based tunnel junction, Nat. Mater. **10**, 347 (2011).

[8] X. Marti, I. Fina, C. Frontera, J. Liu, P. Wadley, Q. He, R. J. Paull, J. D. Clarkson, J. Kudrnovský, I. Turek, J. Kuneš, D. Yi, J-H. Chu, C. T. Nelson, L. You, E. Arenholz, S. Salahuddin, J. Fontcuberta, T. Jungwirth, and R. Ramesh, Room-temperature antiferromagnetic memory resistor, Nat. Mater. **13**, 367 (2014).

[9] S. Y. Huang, X. Fan, D. Qu, Y. P. Chen, W. G. Wang, J. Wu, T. Y. Chen, J. Q. Xiao, and C. L. Chien, Transport Magnetic Proximity Effects in Platinum, Phys. Rev. Lett. **109**, 107204 (2012).

[10] H. Nakayama, M. Althammer, Y.-T. Chen, K. Uchida, Y. Kajiwara, D. Kikuchi, T. Ohtani, S. Geprags, M. Opel, S. Takahashi, R. Gross, G. E. W. Bauer, S. T. B. Goennenwein, and E. Saitoh, Spin Hall Magnetoresistance Induced by a Nonequilibrium Proximity Effect, Phys. Rev. Lett. **110**, 206601 (2013).

[11] Y.-T. Chen, S. Takahashi, H. Nakayama, M. Althammer, S. T. B. Goennenwein, E. Saitoh, and G. E. W. Bauer, Theory of spin hall magnetoresistance (SMR) and related phenomena, J. Phys. Condens. Matter **28**, 103004 (2016).

[12] J. H. Han, C. Song, F. Li, Y. Y. Wang, G. Y. Wang, Q. H. Yang, and F. Pan, Antiferromagnet-controlled spin current transport in SrMnO₃/Pt hybrids, Phys. Rev. B **90**, 144431 (2014).

[13] G. R. Hoogeboom, A. Aqeel, T. Kuschel, T. T. M. Palstra, and B. J. van Wees, Negative spin hall magnetoresistance of Pt on the bulk easy-plane antiferromagnet NiO, Appl. Phys. Lett. **111**, 052409 (2017).

[14] T. Moriyama, N. Matsuzaki, K.-J. Kim, I. Suzuki, T. Taniyama, and T. Ono, Sequential write-read operations in FeRh antiferromagnetic memory, Appl. Phys. Lett. **107**, 122403 (2015).

[15] P. Wadley *et al.*, Electrical switching of an antiferromagnet, Science **351**, 587 (2016).

[16] T. Jungwirth, X. Marti, P. Wadley, and J. Wunderlich Antiferromagnetic spintronics, Nat. Nanotechnol. **11**, 231 (2016).

[17] V. Baltz, A. Manchon, M. Tsoi, T. Moriyama, T. Ono, and Y. Tserkovnyak, Antiferromagnetic spintronics, Rev. Mod. Phys. **90**, 015005 (2018).

[18] A. S. Núñez, R. A. Duine, Paul Haney, and A. H. MacDonald, Theory of spin torques and giant magnetoresistance in antiferromagnetic metals, Phys. Rev. B **73**, 214426 (2006).

[19] H. V. Gomonay and V. M. Loktev, Spin transfer and current-induced switching in antiferromagnets, Phys. Rev. B **81**, 144427 (2010).

[20] O. Gomonay, V. Baltz, A. Brataas, and Y. Tserkovnyak, Antiferromagnetic spin textures and dynamics, Nat. Phys. **14**, 213 (2018).

[21] B. Heinrich, Y. Tserkovnyak, G. Woltersdorf, A. Brataas, R. Urban, and G. E. W. Bauer, Dynamic Exchange Coupling in Magnetic Bilayers, Phys. Rev. Lett. **90**, 187601 (2003).

[22] T. Taniguchi, S. Yakata, H. Imamura, and Y. Ando, Determination of penetration depth of transverse spin current in ferromagnetic metals by spin pumping, Appl. Phys. Express **1**, 031302 (2008).

[23] A. Ghosh, S. Auffret, U. Ebels, and W. E. Bailey, Penetration Depth of Transverse Spin Current in Ultrathin Ferromagnets, Phys. Rev. Lett. **109**, 127202 (2012).

[24] M. K. Marcham, L. R. Shelford, S. A. Cavill, P. S. Keatley, W. Yu, P. Shafer, A. Neudert, J. R. Childress, J. A. Katine, E. Arenholz, N. D. Telling, G. van der Laan, and R. J. Hicken, Phase-resolved x-ray ferromagnetic resonance measurements of spin pumping in spin valve structures, Phys. Rev. B **87**, 180403(R) (2013).

[25] A. A. Baker, A. I. Figueroa, C. J. Love, S. A. Cavill, T. Hesjedal, and G. van der Laan, Anisotropic Absorption of Pure Spin Currents, Phys. Rev. Lett. **116**, 047201 (2016).

[26] P. Merodio, A. Ghosh, C. Lemonias, E. Gautier, U. Ebels, M. Chshiev, H. Béa, V. Baltz, and W. E. Bailey, Penetration depth and absorption mechanisms of spin currents in Ir₂₀Mn₈₀ and Fe₅₀Mn₅₀ polycrystalline films by ferromagnetic resonance and spin pumping, Appl. Phys. Lett. **104**, 032406 (2014).

[27] L. Frangou, S. Oyarzún, S. Auffret, L. Vila, S. Gambarelli, and V. Baltz, Enhanced Spin Pumping Efficiency in

Antiferromagnetic IrMn Thin Films around the Magnetic Phase Transition, Phys. Rev. Lett. **116**, 077203 (2016).

[28] Z. Qiu, J. Li, D. Hou, E. Arenholz, A. T. N'Diaye, A. Tan, K.-i. Uchida, K. Sato, S. Okamoto, Y. Tserkovnyak, Z. Q. Qiu, and E. Saitoh, Spin-current probe for phase transition in an insulator, Nat. Commun. **7**, 12670 (2016).

[29] T. Moriyama, M. Kamiya, K. Oda, K. Tanaka, K.-J. Kim, and T. Ono, Magnetic Moment Orientation-Dependent Spin Dissipation in Antiferromagnets, Phys. Rev. Lett. **119**, 267204 (2017).

[30] A. Kamra, D. M. Polishchuk, V. Korenivski, and A. Brataas, Anisotropic and Controllable Gilbert-Bloch Dissipation in Spin Valves, Phys. Rev. Lett. **122**, 147201 (2019).

[31] Y. Tserkovnyak, A. Brataas, and G. E. W. Bauer, Enhanced Gilbert Damping in Thin Ferromagnetic Films, Phys. Rev. Lett. **88**, 117601 (2002).

[32] Y. Tserkovnyak, A. Brataas, G. E. W. Bauer, and B. I. Halperin, Nonlocal magnetization dynamics in ferromagnetic heterostructures, Rev. Mod. Phys. **77**, 1375 (2005).

[33] S. Mizukami, Y. Ando, and T. Miyazaki, The study on ferromagnetic resonance linewidth for NM/80NiFe/NM (NM = Cu, Ta, Pd and Pt) films, Jpn. J. Appl. Phys. **40**, 580 (2001).

[34] J. Foros, G. Woltersdorf, B. Heinrich, and A. Brataas, Scattering of spin current injected in Pd(001), J. Appl. Phys. **97**, 10A714 (2005).

[35] J Nogués and I. K Schuller, Exchange bias, J. Magn. Magn. Mater. **192**, 203 (1999).

[36] See Supplemental Material at http://link.aps.org/supplemental/10.1103/PhysRevLett.123.247201 for additional FMR data and their analysis, as well as the modeling of the exchange bias in the AF-F_p bilayer as a function of temperature.

[37] R. Jungblut, R. Coehoorn, M. T. Johnson, J. aan de Stegge, and A. Reinders, Orientational dependence of the exchange biasing in molecular-beam-epitaxy-grown

Ni$_{80}$Fe$_{20}$/Fe$_{50}$Mn$_{50}$ bilayers, J. Appl. Phys. **75**, 6659 (1994).

[38] J. Bass and W. P. Pratt, Spin-diffusion lengths in metals and alloys, and spin-flipping at metal/metal interfaces: An experimentalist's critical review, J. Phys. Condens. Matter **19**, 183201 (2007).

[39] S. Chikazumi and T. Oomura, On the origin of magnetic anisotropy induced by magnetic annealing, J. Phys. Soc. Jpn. **10**, 842 (1955).

[40] R. C. O'Handley, *Modern Magnetic Materials: Principles and Applications* (John Wiley and Sons, New York, 2000), p. 437.

[41] F. J. Dyson, Electron spin resonance absorption in metals. II. Theory of electron diffusion and the skin effect, Phys. Rev. **98**, 349 (1955).

[42] A. F. Kravets, D. M. Polishchuk, Y. I. Dzhezherya, A. I. Tovstolytkin, V. O. Golub, and V. Korenivski, Anisotropic magnetization relaxation in ferromagnetic multilayers with variable interlayer exchange coupling, Phys. Rev. B **94**, 064429 (2016).

[43] A. P. Malozemoff, Random-field model of exchange anisotropy at rough ferromagnetic-antiferromagnetic interfaces, Phys. Rev. B **35**, 3679 (1987).

[44] D. Mauri, H. C. Siegmann, P. S. Bagus, and E. Kay, Simple model for thin ferromagnetic films exchange coupled to an antiferromagnetic substrate, J. Appl. Phys. **62**, 3047 (1987).

[45] W. J. Antel, F. Perjeru, and G. R. Harp, Spin Structure at the Interface of Exchange Biased FeMn/Co Bilayers, Phys. Rev. Lett. **83**, 1439 (1999).

[46] Y. Tserkovnyak, A. Brataas, and G. E. W. Bauer, Dynamic stiffness of spin valves, Phys. Rev. B **67**, 140404(R) (2003).

[47] T. Taniguchi and H. Imamura, Enhancement of the Gilbert damping constant due to spin pumping in noncollinear ferromagnet/nonmagnet/ferromagnet trilayer systems, Phys. Rev. B **76**, 092402 (2007).